Phase Transition to Turbulence in Spatially Extended Shear Flows

Lukasz Klotz,[1,2] Grégoire Lemoult,[3] Kerstin Avila,[4,5] and Björn Hof[1,*]
[1]Institute of Science and Technology Austria, Am Campus 1, 3400 Klosterneuburg, Austria
[2]Institute of Aeronautics and Applied Mechanics, Warsaw University of Technology, Nowowiejska 24, 00-665 Warsaw, Poland
[3]CNRS, UMR 6294, Laboratoire Onde et Milieux Complexes (LOMC)53, Normandie Universit, UniHavre, rue de Prony, Le Havre Cedex 76058, France
[4]Faculty of Production Engineering, University of Bremen, Badgasteiner Strasse 1, 28359 Bremen, Germany
[5]Leibniz Institute for Materials Engineering IWT, Badgasteiner Strasse 3, 28359 Bremen, Germany

(Received 2 May 2021; accepted 20 November 2021; published 5 January 2022)

Directed percolation (DP) has recently emerged as a possible solution to the century old puzzle surrounding the transition to turbulence. Multiple model studies reported DP exponents, however, experimental evidence is limited since the largest possible observation times are orders of magnitude shorter than the flows' characteristic timescales. An exception is cylindrical Couette flow where the limit is not temporal, but rather the realizable system size. We present experiments in a Couette setup of unprecedented azimuthal and axial aspect ratios. Approaching the critical point to within less than 0.1% we determine five critical exponents, all of which are in excellent agreement with the $2+1$D DP universality class. The complex dynamics encountered at the onset of turbulence can hence be fully rationalized within the framework of statistical mechanics.

DOI: 10.1103/PhysRevLett.128.014502

With increasing velocity, basic fluid flows undergo a sudden transition from ordered laminar motion to turbulence. Even for the geometrically simplest cases such as pipe, Couette, and channel flow, standard stability theory can neither explain the nature of the transition nor predict its occurrence. To make matters worse, transitional flows erratically switch between perfectly laminar and highly chaotic phases resulting in fluctuation levels that are substantially larger than those encountered in fully turbulent flows at much higher velocities. Despite this apparent complexity, statistical mechanics offers a surprisingly simple explanation for this phenomenon. Macroscopic features of the dynamics bear close resemblance to the universality class of directed percolation [1], probably the most basic phase transition outside of thermal equilibrium.

Directed percolation encompasses a large number of phenomena, including simple epidemic models, fluid flow through porous media, and forest fires [1]. A common feature of all these problems is the competition between an active (e.g., infected) and an absorbing (e.g., susceptible) state governed by a control parameter. Assuming the perspective of turbulence and its eventual decay encountered for decreasing flow speeds, it becomes apparent that the resulting laminar flow qualifies as an absorbing state. Being stable to infinitesimal perturbations, laminar motion persists and the active state, turbulence, cannot arise spontaneously. Based on this analogy Pomeau [2] suggested that the propagation of laminar turbulent fronts may be determined by the critical exponents of directed percolation. This proposition was initially studied for simpler models [3–6] exhibiting spatiotemporal chaos, however, it could not be confirmed for the onset of turbulence in actual fluid flows. In contrast to the expected continuous transition, initial experiments, as well as direct numerical simulations of Couette flow, reported a discontinuous transition [7,8]. A modified analogy to directed percolation (DP) has emerged more recently and resulted from studies of the large scale localized patches that turbulence tends to organize in, close to the critical point. In pipe flow, these so-called puffs have a finite lifetime and their decay is memoryless [9,10]. Prior to decay, puffs can seed new puffs by nearest-neighbor interactions, a process called puff splitting [11], which is equally memoryless [12]. These studies suggest that an individual percolation site is not a turbulent eddy but a macroscopic puff and hence a structure that is more than an order of magnitude larger than sites were previously expected to be. A further difference to the original DP analogy is that this transition does not account for the eventual emergence of fully turbulent flow, which only results from a distinct transition at higher Re [13,14]. Puffs consist of a short turbulent upstream part (5D in length) and an elongated quiescent leading edge (20D) across which the profile recovers from a plug to a more parabolic shape. This profile recovery sets the minimum puff spacing [15,16]. Consequently, the analogous state to a fully occupied lattice in DP is a dense pattern of distinct puffs, not fully turbulent flow. The dynamics of the process are governed by the decay and splitting rates of puffs and, in the proximity of the critical point, on average, a puff travels 10^7 diameters downstream before either event

occurs [12]. While various numerical studies determined directed percolation exponents for models of varying complexity (including direct numerical simulations) [14,17–22], measurements in actual fluid flows have to resolve both, the large spatial and temporal scales.

So far, this has only been possible in an experimental setting where, like in pipe flow, the dynamics of turbulent sites is confined to a single spatial dimension [23]. The circular Couette geometry chosen in that study and the resulting periodic boundary conditions allowed us to observe pufflike turbulent structures for sufficiently large times (order of 10^6 advective units; note that at the critical point of Couette flow the decay and splitting times are about two decades smaller than those in pipes [24]). In this case, indeed a continuous transition was reported with exponents closely matching those of directed percolation in $1+1$ dimensions. The purpose of the present study is to establish if the DP analogy observed for flows extended in one dimension carries over to planar flows, where turbulence arranges in stripe patterns that proliferate in two dimensions. While for the Waleffe model the onset of sustained turbulent stripes has been shown to closely agree with the $2+1$D DP universality class [20], experimental evidence is missing.

At odds with the large scales [see Fig. 1(b) for a comparison of the temporal and spatial scales] required for the investigation of the transition type described above, a recent experimental study of channel flow [25] reported a fundamentally different DP analogy. In that case, the inlet was forced to be fully turbulent and the flow was investigated in a comparably small experimental domain [see vertical dimension of red square in Fig. 1(b)] and for short observation times (see horizontal extend of red square compared to the 3 orders of magnitude larger stripe splitting times [26], red dashed line). However, in this case, the eventual flow never settled to the large scale stripe patterns that have been reported in other studies of channel flow [27–30]. Moreover, recent numerical and experimental studies of channel flow [28–31] could not confirm the phase transition point suggested in [25]. Instead, in these more recent studies, turbulent stripes were observed to persist to significantly lower Reynolds numbers, suggesting that in [25] flows may have not reached the eventual statistical steady state and that the observed dynamics were transient, which would also explain the difference in the structures observed. It is also noteworthy that [25] obtained nonzero turbulent fractions below what they suggested as a critical point. While the authors attributed the nonvanishing turbulent fraction to finite size effects, a finite system size classically has the opposite effect and causes turbulent fractions to already reach zero (i.e., a discontinuity) slightly above critical, provided that observation times are sufficient.

In the present investigation of cylindrical Couette flow, the periodic boundary conditions ensure that flow patterns

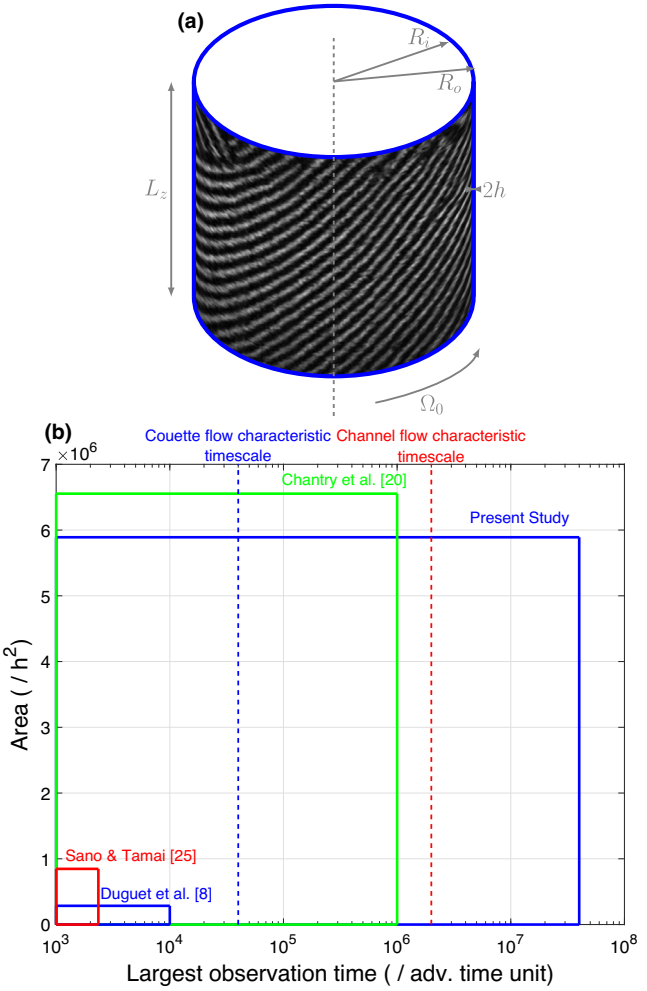

FIG. 1. (a) Schematic of experimental apparatus. (b) Typical test section sizes and timescales covered in previous studies when compared to the present experiment. Note that the observation time is defined as the maximum time over which the evolution of a flow pattern can be investigated in a comoving frame. It hence does not necessarily coincide with (and often is far shorter than) the recording time.

can be investigated for arbitrarily long times. To ensure that the results are not affected by finite size effects [32,33], a very small gap size ($2h$) had to be chosen. In contrast to [23], our system is not only extended in the azimuthal direction but equally in the spanwise (or axial) direction, and hence flow patterns are expected to be two-dimensional and consist of stripes and not of puffs. Given that the minimum spacing between turbulent stripes in Couette flow is approximately $70h$, aspect ratios in excess of a thousand h are required to accommodate flow patterns comprising sufficient stripe numbers (i.e., a sufficient number of sites).

The experiment consists of a pair of concentric, high precision cylinders, an outer glass cylinder (with an inner diameter of 150 mm), and an inner (hollow) stainless steel cylinder (with an outer diameter of 149.52 mm), resulting in a gap size of $2h = 240$ μm (Fig. 1). Given the azimuthal

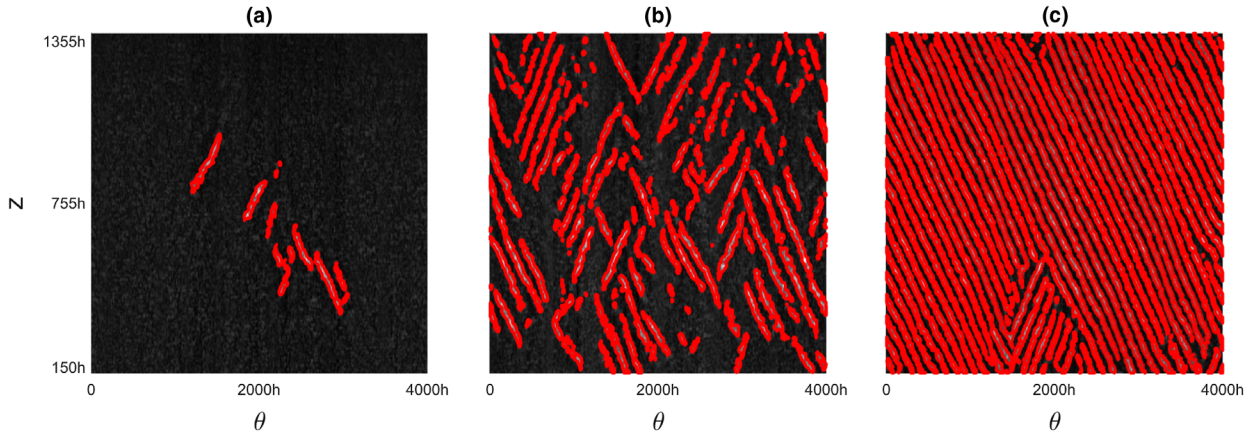

FIG. 2. Turbulent stripes in the axial-azimuthal cross section. Flow visualizations for (a) Re = 331, (b) Re = 333, and (c) Re = 349. Turbulent phase is marked by red contours. The laminar regions (black) expand as the Reynolds number is decreased and stripes become sparse.

circumference $C = 471.225$ mm and the cylinder length of $H = 180$ mm, the azimuthal (C/h) and axial (H/h) aspect ratios are 3927 and 1500, respectively. While the outer cylinder is held in place by air bearings (constraining it in the radial and the axial direction), the inner one is held by a hollow shaft that allows one to circulate temperature controlled fluid through the cylinder core and hence to temperature control the experiment (with a precision of 0.02 K). The gap between the two cylinders is filled with ethanol (99%) and, in addition, a small amount (mass concentration $C_m \approx 5 \times 10^{-4}$) of micron sized aluminum flakes (Eckart PCR1100) is added to the fluid to visualize the flow patterns. The latter were recorded using two line cameras (Basler spL 4096) (see also [23] and Supplemental Material [34] for the azimuthal reconstruction from a time series). The flow is driven by the rotation of the outer cylinder with angular velocities ranging from 1000 to 1300 rpm. The gap uniformity during outer cylinder rotation (i.e., relative variation around the mean value) has been measured to be better than ± 6 μm and the eccentricity between the inner and the outer cylinder is less than 5 μm, as described in detail in the Supplemental Material [34]. The control parameter, the Reynolds number ($\mathrm{Re} = \Omega_o R_o h/2\nu$, where Ω_o is the angular velocity, R_o is the radius of the outer cylinder, and ν is the fluids kinematic viscosity) could be controlled to better than $\Delta\mathrm{Re} = \pm 0.5$.

Unless perturbed, the flow remains laminar up to Reynolds numbers exceeding 400, confirming the concentricity and overall high accuracy of the setup. It is noted that, in early prototypes of the experiment, misalignments of the cylinders had been found to trigger turbulence at significantly lower Re. In order to determine the critical point, where turbulence first becomes sustained, the laminar flow must be perturbed initially. In our case, this was achieved by a sudden increase to a higher Reynolds number ($\mathrm{Re} \approx 520$), followed by a quench to the lower target Reynolds number. Here the flow would settle to a state of spatiotemporal intermittency, which was then left to stabilize for 10^7 advective time units (see also Fig. S5 in the Supplemental Material [34]) to approach its statistical steady state. Subsequently, image time series were recorded for at minimum 10^7 (closer to critical for up to 4×10^7) advective time units [see Fig. 1(b)]. In accordance with the above suggested DP analogy and as confirmed experimentally for pipe flow [35], the temporal transients (blue dataset in Fig. S5) are hence substantially larger than the splitting and decay times of single stripes (blue dashed line in Fig. S5). Toward the higher end of the investigated Reynolds number interval, the measurement volume is densely packed with turbulent stripes [see Fig. 2(c), $\mathrm{Re} = 349$] and the stripe spacing of the order of $\lambda \approx 70h$ is the smallest spacing stripes can assume [16,36]. In the DP context, λ therefore corresponds to the size of a single site and is the natural length scale of the problem (see also Fig. S4 and the discussion in the Supplemental Material [34]). With decreasing Reynolds number, the density of stripes and hence the turbulent fraction, which is the order parameter, decrease [from Figs. 2(c) to 2(a)]. As shown in Fig. 3(a), the TF decreases continuously as the critical point is approached [the TF is shown as a function of the reduced Reynolds number $\epsilon = (\mathrm{Re} - \mathrm{Re}_c)/\mathrm{Re}_c$].

More precisely, the TF is found to scale with a power law, i.e., $\mathrm{TF} \sim \epsilon^{\beta}$. The best fit [red dashed line in Fig. 3(a)] results in a value of $\mathrm{Re}_c = 330.0 \pm 0.5$, $\beta = 0.59 \pm 0.03$. This experimentally obtained value of β is in excellent agreement with the corresponding critical exponent of the directed percolation universality class in two spatial dimensions (2 + 1D DP), which is $\beta^{\mathrm{DP}} = 0.583$ [shown by the black line in Fig. 3(a)]. In addition to the power-law scaling of TF, directed percolation is characterized by distinct scaling relations for the correlation length and correlation time in the vicinity of the critical point. Hence, the corresponding two correlation exponents establish if the transition falls into this universality class. To test this, we

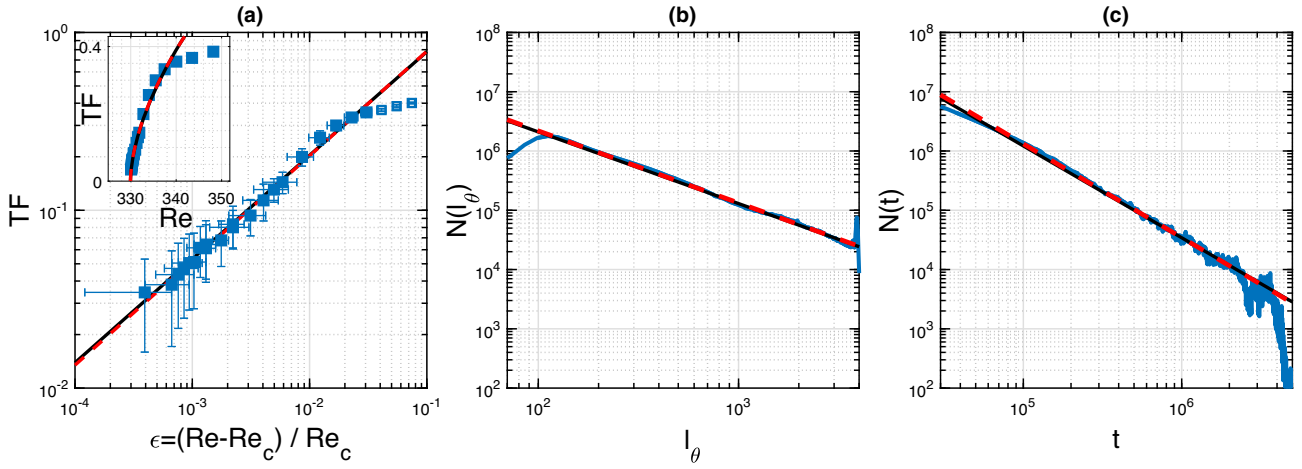

FIG. 3. Order parameter and critical exponents. (a) Power-law dependence of turbulent fraction (TF) (blue squares) on the distance from the critical Reynolds number $\epsilon = (\mathrm{Re} - \mathrm{Re}_c)/\mathrm{Re}_c$ shown in log-log (linear scale in inset). The distributions of the azimuthal (streamwise) sizes of the laminar gaps $N(l_\theta)$ and the laminar time intervals $N(\tau)$ close to the critical point ($\mathrm{Re} = 331$) are illustrated by blue curves in (b) and (c), respectively. In each panel, the red dashed lines illustrate the best fit [(a) $\mathrm{TF} \sim \epsilon^\beta$ with $\beta = 0.59$; (b) $N(l_\theta) \sim l^{-\mu_\perp}$ with $\mu_\perp = 1.22 \pm 0.02$; (c) $N(\tau) \sim \tau^{-\mu_\parallel}$ with $\mu_\parallel = 1.58 \pm 0.03$] and black solid lines correspond to theoretical prediction for $(2+1)$DP universality class ($\beta^{\mathrm{DP}} = 0.58, \mu_\perp^{\mathrm{DP}} = 1.21, \mu_\parallel^{\mathrm{DP}} = 1.55$).

next investigated the sizes of the laminar gaps along the azimuthal direction $N(l_\theta)$ in the vicinity of the critical point. As shown in Fig. 3(b), the gap size distribution also follows a power law and the flow is hence scale invariant [24]. Finally, in Fig. 3(c), we plot the duration of the laminar gaps in time $N(t)$ and again a power law is obtained. The corresponding critical exponents for the spatial and temporal gap distributions (best fits are given by the red dashed lines) are found to be $\mu_\perp^\theta = 1.22 \pm 0.02$ and $\mu_\parallel = 1.58 \pm 0.03$, while the values for directed percolation (black lines in the respective figure panels) are $\mu_\perp^{\mathrm{DP}} = 1.204$ and $\mu_\parallel^{\mathrm{DP}} = 1.549$, and hence the values are in close agreement.

While these three exponents provide sufficient evidence that the transition to turbulence belongs to the $2+1$D DP universality class, additional exponents can be obtained in separate experiments and hence allow an independent confirmation. By considering the laminar gap size distributions at various distances from the critical point, the corresponding characteristic length scale has been determined as a function of the control parameter (see Fig. 4 and Supplemental Material [34]). This procedure has been carried out separately for the gap spacings in the azimuthal and axial directions and for the gap durations (temporal gaps). In DP, the corresponding correlation length and time diverge with characteristic power laws (black lines in Fig. 4) as the critical point is approached. The experimental

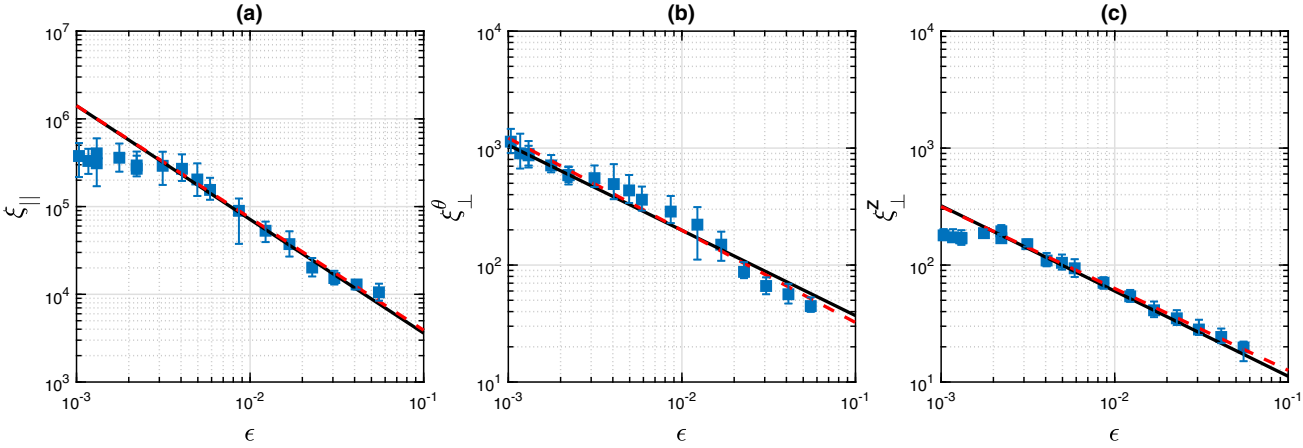

FIG. 4. Correlation exponents at the phase transition. Dependence of correlation time [(a) $\xi_\parallel$] and correlation lengths [(b) $\xi_\perp^\theta$; (c) $\xi_\perp^z$] on control parameter ϵ. In each panel, the red dashed line corresponds to the best fit [(a) $\xi_\parallel \sim \epsilon^{-\nu_\parallel}$ with $\nu_\parallel = 1.28$; (b) $\xi_\perp^\theta \sim \epsilon^{-\nu_\perp^\theta}$ with $\nu_\perp^\theta = 0.79$; (c) $\xi_\perp^z \sim \epsilon^{-\nu_\perp^z}$ with $\nu_\perp^z = 0.70$] and black solid lines correspond to the theoretical predictions for the $(2+1)$DP universality class ($\nu_\parallel = 1.296, \nu_\perp^{\mathrm{DP}} = 0.729$).

data for Couette flow (blue symbols in Fig. 4) are in close agreement with the DP prediction. The fitted power laws (red lines) diverge at $\mathrm{Re}_c = 330.0$ [the critical point determined from the measurements in Fig. 3(a)].

The transition to turbulence has been under scientific scrutiny for over a century and, although directed percolation has been suggested as a possible solution to the problem three decades ago, direct evidence has only recently been obtained for simplified geometries. The canonical cases, pipe, Couette, and channel flow appeared out of reach due to the enormous temporal and spatial scales that dominate the transition process. Resolving these scales in pipe and channel flows, where turbulent structures move at the mean flow speed, would require experiments of lengths easily exceeding 10^3 km. Couette flow, on the other hand, can be realized in a circular geometry with periodic boundary conditions and hence appears a more feasible target. Nevertheless, the required aspect ratios pose a formidable hurdle. In the present case, the fluid had to be confined to a 240 μm thin sheet with the overall physical dimensions closely matching those of a page of A4 paper (10 pt). The velocity difference across the thin fluid film, on the other hand, had to be increased beyond 10 m/s to trigger turbulence. The difficulty in measuring critical exponents is not specific to turbulence, but more broadly applies to nonequilibrium systems. Although directed percolation is believed to be relevant to numerous problems in diverse areas of the natural sciences [1], experimental verification of this universality class [37] has been a longstanding problem [38]. The transition to turbulence offers the first example that is of broad practical relevance.

We thank T. Menner, T. Asenov, P. Maier, and the Miba machine shop of IST Austria for their valuable support in all technical aspects. We thank Marc Avila for comments on the Letter. This work was supported by a grant from the Simons Foundation (662960, B. H.). We acknowledge the European Research Council under the European Union's Seventh Framework Programme (FP/2007-2013)/ERC Grant Agreement No. 306589 for financial support. K. A. acknowledges funding from the Central Research Development Fund of the University of Bremen, Grant No. ZF04B /2019/FB04 Avila Kerstin ("Independent Project for Postdocs"). L. K. was supported by the European Unions Horizon 2020 research and innovation program under the Marie Skłodowska-Curie Grant Agreement No. 754411.

*bhof@ist.ac.at

[1] H. Hinrichsen, Adv. Phys. **49**, 815 (2000).
[2] Y. Pomeau, Physica (Amsterdam) D **23**, 3 (1986).
[3] K. Kaneko, Prog. Theor. Phys. **74**, 1033 (1985).
[4] H. Chaté and P. Manneville, Phys. Rev. Lett. **58**, 112 (1987).
[5] H. Chaté and P. Manneville, Physica (Amsterdam) D **32**, 409 (1988).
[6] J. Rolf, T. Bohr, and M. H. Jensen, Phys. Rev. E **57**, R2503 (1998).
[7] S. Bottin, F. Daviaud, P. Manneville, and O. Dauchot, Europhys. Lett. **43**, 171 (1998).
[8] Y. Duguet, P. Schlatter, and D. S. Henningson, J. Fluid Mech. **650**, 119 (2010).
[9] B. Hof, J. Westerweel, T. M. Schneider, and B. Eckhardt, Nature (London) **443**, 59 (2006).
[10] B. Hof, A. de Lozar, D. J. Kuik, and J. Westerweel, Phys. Rev. Lett. **101**, 214501 (2008).
[11] D. Moxey and D. Barkley, Proc. Natl. Acad. Sci. U.S.A. **107**, 8091 (2010).
[12] K. Avila, D. Moxey, A. de Lozar, M. Avila, D. Barkley, and B. Hof, Science **333**, 192 (2011).
[13] D. Barkley, B. Song, V. Mukund, G. Lemoult, M. Avila, and B. Hof, Nature (London) **526**, 550 (2015).
[14] D. Barkley, J. Fluid Mech. **803** (2016).
[15] B. Hof, A. de Lozar, M. Avila, X. Tu, and T. Schneider, Science **327**, 1491 (2010).
[16] D. Samanta, A. d. Lozar, and B. Hof, J. Fluid Mech. **681**, 193 (2011).
[17] D. Barkley, Phys. Rev. E **84**, 016309 (2011).
[18] M. Sipos and N. Goldenfeld, Phys. Rev. E **84**, 035304(R) (2011).
[19] H.-Y. Shih, T.-L. Hsieh, and N. Goldenfeld, Nat. Phys. **12**, 245 (2016).
[20] M. Chantry, L. S. Tuckerman, and D. Barkley, J. Fluid Mech. **824** (2017).
[21] P. Manneville and M. Shimizu, Entropy **22**, 1348 (2020).
[22] K. Takeda, Y. Duguet, and T. Tsukahara, Entropy **22**, 988 (2020).
[23] G. Lemoult, L. Shi, K. Avila, S. V. Jalikop, M. Avila, and B. Hof, Nat. Phys. **12**, 254 (2016).
[24] L. Shi, M. Avila, and B. Hof, Phys. Rev. Lett. **110**, 204502 (2013).
[25] M. Sano and K. Tamai, Nat. Phys. **12**, 249 (2016).
[26] S. Gome, L. S. Tuckerman, and D. Barkley, Phys. Rev. Fluids **5**, 083905 (2020).
[27] T. Tsukahara, Y. Seki, H. Kawamura, and D. Tochio, arXiv:1406.0248.
[28] X. Xiong, J. Tao, S. Chen, and L. Brandt, Phys. Fluids **27**, 041702 (2015).
[29] M. Shimizu and P. Manneville, Phys. Rev. Fluids **4**, 113903 (2019).
[30] C. S. Paranjape, Ph.D. thesis, Institute of Science and Technology Austria, 2019.
[31] J. J. Tao, B. Eckhardt, and X. M. Xiong, Phys. Rev. Fluids **3**, 011902(R) (2018).
[32] K. Avila and B. Hof, Rev. Sci. Instrum. **84**, 065106 (2013).
[33] K. Avila and B. Hof, Entropy **23**, 58 (2021).
[34] See Supplemental Material at http://link.aps.org/supplemental/10.1103/PhysRevLett.128.014502 for a more detailed description of the experimental set up and procedures as well as for a discussion of the experimental requirements for a characterization of the phase transition.
[35] V. Mukund and B. Hof, J. Fluid Mech. **839**, 76 (2018).
[36] A. Prigent, G. Grégoire, H. Chaté, O. Dauchot, and W. van Saarloos, Phys. Rev. Lett. **89**, 014501 (2002).
[37] K. A. Takeuchi, M. Kuroda, H. Chaté, and M. Sano, Phys. Rev. Lett. **99**, 234503 (2007).
[38] H. Hinrichsen, Braz. J. Phys. **30**, 69 (2000).